Effect of Aromatic Ring Substitution on the Optical Properties, Emission Dynamics, and Solid-State Behavior of Fluorinated Oligophenylenevinylenes

Bernd Strehmel,[†] Ananda M. Sarker,[†] John H. Malpert,[†] Veronika Strehmel,[‡] Holger Seifert,[§] and Douglas C. Neckers*,[†]

Contribution from the Center for Photochemical Sciences,[1] Bowling Green State University, Bowling Green, Ohio 43403, Institute for Technical and Macromolecular Chemistry, Martin-Luther-University Halle-Wittenberg, Geusaer Strasse, D-06217 Merseburg, Germany, and Institute of Physical and Theoretical Chemistry, Humboldt University of Berlin, Bunsenstrasse 1, D-10117 Berlin, Germany

Received September 16, 1998

Abstract: Several substituted oligophenylenevinylenes were synthesized using the Wittig−Horner−Emmons reaction to produce the trans isomers. Optical properties of these compounds were evaluated using absorption and steady-state fluorescence spectroscopy. Fluorescence quantum yields, Φ_f, decrease with increasing solvent polarity and approach unity in nonpolar solvents in the case of substituted *trans,trans*-1,4-bis[2-(2′,5′-difluoro)-phenylethenyl]benzenes and *trans,trans*-1,4-bis[2-(2′,5′-dialkoxy)phenylethenyl)-2,3,5,6-tetrafluorobenzenes. The compounds show a strong solvatochromic shift as a function of solvent polarity, yielding a slope of −13 300 cm^{-1} according to the Lippert−Mataga equation and indicating the emission of an additional charge-transfer species. A two-state reaction model was confirmed for *trans,trans*-1,4-bis[2-(2′,5′-dialkoxy)phenylethenyl)-2,3,5,6-tetrafluorobenzene (**6d**) in different solvents by time-correlated single-photon counting using global analysis. A dependence of the kinetic data on solvent polarity was found (global fitted decay times in picoseconds for τ_1 and τ_2: 381/1281 in *n*-hexane; 101/1590 in toluene; 27/2974 in acetonitrile). Investigations of the solid state showed liquid crystalline behavior for **6d** and for *trans,trans*-1,4-bis[2-(2′,5′-difluoro)phenylethenyl]-2,5-diheptyloxybenzene (**3b**). This was confirmed by polarization microscopy and thermal analysis. Both the long alkoxy chains and fluorine substitution are responsible for the formation of mesophases. Photoluminescence studies of **3b** and **6d** in the solid state indicated an intense emission that was yellow for **3b**.

Introduction

Polyphenylenevinylene (PPV) derivatives have received a considerable amount of attention due to their applications in electroluminescence (EL) devices.[2,3] A most challenging task in this field is to optimize the photophysical behavior of the PPVs to achieve high quantum efficiencies of both photo- and electroluminescence. The introduction of various alkyl or alkoxy substituents in the phenylene ring provides soluble materials that allow one to tune the emission properties.[3,4] The attachment of electron-withdrawing groups on the vinyl group, particularly cyano substituents, results in an increase of luminescence quantum.[5,6] Recently, the attachment of fluorine substituents on the phenylene ring showed considerable red-shifted EL.[7] Fluorine might be expected to have important electronic

implications on PPV light emission, as well as in stabilizing the PPV backbone against oxidation.[8]

Spectra of donor−acceptor-type compounds revealed an additional relaxation in the excited state described as an interchain excimer-state emission.[9] Such polymers are substituted by electron-donating and -withdrawing groups, leading to fluorescence that depends on environment. This was recently confirmed for a series of cyano- and alkoxy-substituted oligophenylenevinylenes.[6] On the other hand, no significant difference of the emission was reported for PPVs having only alkoxy group substitution in ordinary solvents, gels, films, and blends.[10]

Fluorinated oligophenylenevinylenes having different alkyl or alkoxy groups on the aryl ring should be useful in addressing the relationship between luminescence and structure. Advantageously, these oligomers allow examination of optical properties in solution because they are more soluble than the unsubstituted analogues. In addition, fluorine is a strong electron-withdrawing group, while methyl and methoxy are donor groups. Therefore, compounds having such functional groups should help us to understand the behavior of oligo-

[†] Bowling Green State University.
[‡] Martin-Luther-University Halle-Wittenberg.
[§] Humboldt University of Berlin.
(1) Contribution no. 375 from the Center for Photochemical Sciences.
(2) Burroughes, J. H.; Bradley, D. D. C.; Brown, A. R.; Marks, R. N.; Mackay, K.; Friend, R. H.; Burn, P. L.; Holmes, A. B. *Nature* **1990,** *347,* 539.
(3) Kraft, A.; Grimsdale, A. C.; Holmes, A. B. *Angew. Chem., Int. Ed.* **1998,** *37,* 402.
(4) Burn, P. L.; Holmes, A. B.; Kraft, A. B.; Bradley, D. D. C.; Brown, A. R.; Friend, R. H.; Gymer, R. W. *Nature* **1992,** *356,* 47.
(5) Greenham, N. C.; Moratti, S. C.; Bradley, D. D. C.; Friend, R. H.; Holmes, A. B. *Nature* **1993,** *365,* 628.
(6) Oelkrug, D.; Tompert, A.; Gierschner, J.; Egelhaaf, H.-J.; Hanack, M.; Hohloch, M.; Steinhuber, E. *J. Phys. Chem. B* **1998,** *102,* 1902.

(7) Gurge, R. M.; Sarker, A. M.; Lahti, P. M.; Hu, B.; Karasz, F. E. *Macromolecules* **1997,** *30,* 8286.
(8) Scurlock, R. D.; Wang, B.; Ogilby, P. R.; Sheats, J. R.; Clough, R. L. *J. Am. Chem. Soc.* **1995,** *117,* 10194.
(9) Harrison, N. T.; Baigent, D. R.; Samual, I. D. W.; Friend, R. H. *Phys. Rev. B* **1996,** *53,* 15815.
(10) Smilowitz, L.; Hays, A.; Heeger, A. J.; Wang, G.; Bowers, J. E. *J. Chem. Phys.* **1993,** *98* (8), 6504.

Scheme 1. General Route for the Synthesis of Compounds **3a−d** and **6a−d** According to a Wittig−Horner−Emmons Reaction
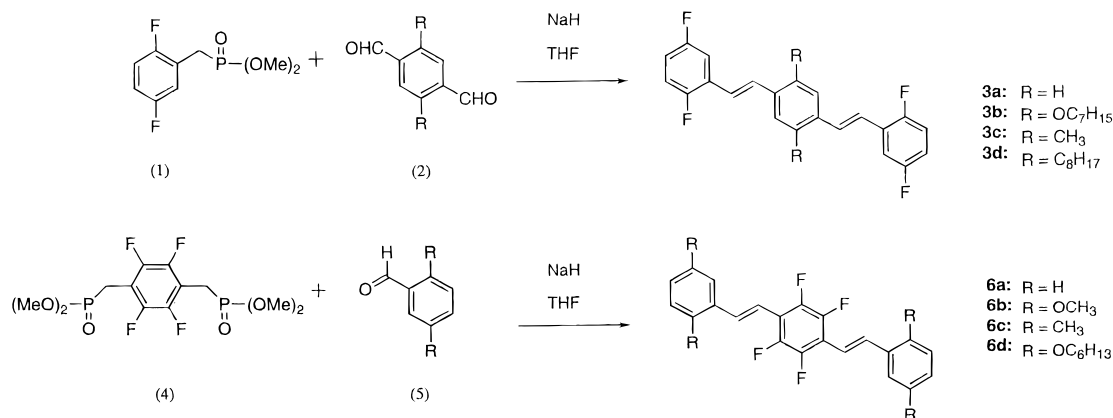
phenylenevinylenes in the excited state. Replacement of the short alkyl or alkoxy groups by long chains allows the examination of self-assembling effects[11] that can lead to the formation of ordered structures in the solid state.

Liquid crystalline behavior has been previously reported for oligophenylenevinylenes. Specifically, mesomorphism has been found in poly(2,5-dialkoxy-1,4-phenylene-2,5-thiophene)s, poly-(2,5-dialkoxy-phenylenevinylene), and poly(*p*-phenylene),[12] where smectic and nematic textures were observed. The localization of the phase transition decreases with increasing chain length.[12] Replacement of the ethylenic unit by ethynyl groups yields polymers with ordered structures considered as rigid rods.[13] The phase transition from the liquid crystalline to the isotropic state in oligophenylenevinylenes having alkyl side chains has been investigated by differential scanning calorimetry, nuclear magnetic resonance, and polarization microscopy.[14] A typical Schlieren texture was observed, indicating a nematic phase transition. NMR analysis showed a rotation of the rigid backbone along the molecular axis in the liquid crystalline phase. A study of the activation energies for C−H bond orientation indicated that the alkyl chains were considered as "bound solvent". Ordered textures were observed below the melting point of the neat material for cast films of *n*-octyloxy-substituted oligo(*p*-phenylenevinylene).[15] X-ray analysis of cast films upon heating indicated an enhanced molecular orientation. The layers had a distance of about 15 Å and were aligned parallel to the surface.

The substitution of the aromatic ring with fluorine should lead to π-stacking, as previously reported for *trans,trans*-1,4-bis(2-phenylethenyl)-2,3,5,6-tetrafluorobenzene. π-Stacking is responsible for the [2 + 2] photodimerization of this compound in the solid state.[16] Substitution with chlorine,[17] fluorine,[18] or alkoxyaryl groups[19] can direct specific packing in the crystal. Moreover, donor−acceptor interactions are important for molecular alignment of photoreactions in the solid state.[20] Finally, stacking can contribute to the formation of discotic phases in liquid crystalline materials.[21]

The goal of the current work was to understand the photochemistry of the model compounds in ordinary solvents and to find correlations between the structure and the properties in combination with their fluorescence emission. The influence of substitution on the absorption and emission behavior was examined by selective modification of the substituents, focusing on the variation of donor strength and position on the chain. Some optical properties were studied using absorption and steady-state fluorescence in dilute solution. Under these conditions, aggregation effects that would complicate kinetics in the excited state can be eliminated. Furthermore, global analysis

was applied to evaluate the emission dynamics[22−26] using a standard time-correlated single-photon counting technique.[27] Finally, differential scanning calorimetry (DSC), polarization microscopy, and steady-state fluorescence were combined to characterize the solid-state properties. These investigations were addressed to show the correlations between structure and the resulting thermal properties. Polarization microscopy was used to investigate which compounds show birefringence in the molten state. Birefringence is an indication for ordered phases in the melt that can lead to unexpected red shifts in fluorescence in the solid state.

Results and Discussion

Synthesis. Synthesis of the *trans,trans*-1,4-bis[2-(2′,5′-difluoro)phenylethenyl]benzenes (**3a−d**) began with the commercially available α-bromo-2,5-difluorotoluene. Treatment with trimethyl phosphite provided the corresponding phosphonate ester (**1**), Scheme 1. The aryl dialdehydes (**2**) were made via the corresponding dibromides upon metalation with *n*-BuLi and

(11) Ullmann, A. *An Introduction to Ultrathin Organic Films: From Langmuir Blodgett to Self-Assembly*; Academic Press: Boston, 1991.

(12) Yu, L.; Bao, Z. *Adv. Mater.* **1994**, *6*, 156.

(13) Moroni, M.; Le Moigne, J.; Luzzati, S. *Macromolecules* **1994**, *27*, 562.

(14) Zhu, W.; Li, W.; Yu, L. *Macromolecules* **1997**, *30*, 6274.

(15) Bouwer, H. J.; Krasnikow, V. V.; Pham, T. A.; Gill, R. E.; Van Hutten, P. F.; Hadziioannou, G. *Chem. Phys.* **1998**, *227*, 65.

(16) Coates, G. W.; Dunn, A. R.; Henling, M. L.; Ziller, J. W.; Lobkovsky, E. B.; Grubbs, R. H. *J. Am. Chem. Soc.* **1998**, *120*, 3641.

(17) Sarma, J. A. R. P.; Desiraju, G. R. *J. Chem. Soc., Chem. Commun.* **1984**, 145.

(18) Vishnumurthy, K.; Row, T. N. G.; Venkatesan, K. *J. Chem. Soc., Perkin Trans. 2* **1997**, 615.

(19) Desiraju, G. R.; Kamala, R.; Kumari, B. H.; Sarma, J. A. R. P. *J. Chem. Soc., Perkin Trans. 2* **1984**, 181.

(20) Sharma, C. V. K.; Panneerselvam, K.; Shimoni, L.; Katz, H.; Carrell, H. L.; Desiraju, G. R. *Chem. Mater.* **1994**, *6*, 1282.

(21) Samulski, E. *The Mesomorphic State*. In *Physical Properties of Polymers*; Mark, J. E., Eisenberg, A., Graessley, W. A., Mandelkern, L., Samulski, E., Koenig, J. L., Wignall, G., Eds.; American Chemical Society: Washington, DC, 1993.

(22) van Stam, J.; De Schryver, F. C.; Boens, N.; Hermans, B.; Jerome, R.; Trossaert, G.; Goethals, E.; Schacht, E. *Macromolecules* **1997**, *30*, 5582.

(23) Amelot, M.; Boens, N.; Andriessen, R.; Van den Bergh, V.; De Schryver, F. C. *J. Phys. Chem.* **1991**, *95*, 2041.

(24) Khalil, M. M. H.; Boens, N.; Van der Auerwaer, M.; Ameloot, M.; Andriessen, R.; Hofkens, J.; De Schryver, F. C. *J. Phys. Chem.* **1991**, *95*, 9375.

(25) Strehmel, B.; Seifert, H.; Rettig, W. *J. Phys. Chem. B* **1997**, *101*, 2232.

(26) Beechem, J. M.; Gratton, E.; Amelot, M.; Knutson, J. R.; Brand, L. In *Topics in Fluorescence Spectroscopy;* Lakowicz, J. R., Ed.; Plenum Press: New York, 1991; Vol. 2, p 241.

(27) O'Connor, D. V.; Phillips, D. *Time Correlated Single Photon Counting*; Academic Press: London, 1984.

Table 1. Absorption (Maximum of Absorption, λ_a) and Emission Data (Maximum of Fluorescence, λ_f, and Fluorescence Quantum Yield, Φ_f) for **3a–c** and **6a–d** in Toluene and Acetonitrile

compound	solvent	λ_a (nm)	λ_f (nm)	Φ_f
3a	toluene	360	396	0.97
	CH$_3$CN	354	393	0.48
3b	toluene	398	456	0.93
	CH$_3$CN	392	459	0.55
3c	toluene	358	406	0.91
	CH$_3$CN	346	407	0.33
6a	toluene	354	388	0.38
	CH$_3$CN	346	386	0.07
6b	toluene	386	441	0.91
	CH$_3$CN	380	510	0.72
6c	toluene	352	402	0.29
	CH$_3$CN	344	402	0.05
6d	toluene	386	445	0.99
	CH$_3$CN	378	518	0.69

quenching with *N,N*-dimethylformamide. In the cases where R = alkyl, the yields were often low due to incomplete conversion to the aryl dianion providing mixtures of the desired dialdehydes (**4**) along with the monoaldehyde. These compounds could be separated by column chromatography. Finally, a Wittig–Horner–Emmons olefination procedure[28,29] provided the *trans, trans*-1,4-bis[2-(2′,5′-difluoro)phenylethenyl]benzene compounds (**3a–d**) in good yields. The stereochemistry of the trans double bond was established by the coupling constant of the vinylic protons in the ^{1}H NMR ($J = 15-17$ Hz) and by bands in the IR (970 cm^{-1}), typical for trans-substituted polyphenylene-vinylenes.

The diphosphonate ester (**4**) was made from the corresponding tetrafluorobenzyl dibromide, and the aldehydes (**5**) were commercially available or easily synthesized by standard organic procedures. Once again, characterization of the trans double bond was made via ^{1}H NMR and IR spectroscopy. No cis conformer was detected. Only one spot was observed in the thin-layer chromatogram.[30]

Absorption and Steady-State Fluorescence. Aggregation effects that are usually dominant in cast films of the neat compound were excluded by photophysical measurements.[6,16,31] In general, a dependence of the absorption maximum as a function of fluorine, alkyl, or alkoxy substitution was found for **3a–d** and **6a–d**, see Table 1. Compounds with alkoxy substituents (**3b**, **6b**, **6d**) showed the largest bathochromic shift and two well-separated bands above 300 nm. The large molar absorption coefficients (about 40 000 M^{-1} cm^{-1}) indicate the dominance of $\pi-\pi^*$ transitions, and additional shoulders or smaller contributions were found in the spectra. A slight hypsochromic shift of the absorption maximum was observed in polar solvents for all compounds. The results are summarized in Table 1.

Brief quantum mechanical studies at a semiempirical level for **3a**, **3c**, **6a**, **6b**, **6c** and a modified compound for **3b** (substituted with methoxy groups instead of heptyloxy groups) indicate a localization of the electron in the donor part (represented by alkoxy substitution) for the occupied orbital HOMO−1. The unoccupied orbital LUMO+1 clearly shows localization of the electron in the acceptor part (represented for example by the fluorine substitution). All compounds are highly symmetrical (C_{2h}) and are planar without any indication for a pretwist of a phenyl group. The largest charge separation was found for **6b**.

Fluorescence quantum yields (Table 1) show a dependence on solvent polarity, and the highest values were found in nonpolar solvents, where the yields approach 1. A consistent decrease in Φ_f was found with increasing solvent polarity. Triplet states have minor importance. Furthermore, high fluorescence quantum yields in toluene are consistent with results published about intramolecular charge transfer (ICT) in several donor–acceptor-substituted compounds.[32–38]

Compounds **6b** and **6d**, with tetraalkoxy and perfluoro substitution, show an unexpected strong shift of the fluorescence maximum in ordinary solvents. Replacing the alkoxy group with methyl groups as in **6c** leads to little shift in fluorescence. The fluorescence spectra obtained for **3a**, **3c**, **6a**, and **6c** show no significant shift of the emission maximum, nor did the peaks change their shape. The spectrum is almost structured, showing a change of the fluorescence quantum yield as a function of solvent polarity. On the other hand, a Stokes shift of more than 3000 cm^{-1} was measured for **6b** and **6d** upon changing from a nonpolar to polar medium (toluene → acetonitrile), see Figure 1. Compound **3b,** which possesses dialkoxy substitution on the middle aryl ring and difluoro substitution on the terminating aromatic units, shows only a small shift of the emission spectra, but the spectral shift is dependent upon the polarity of the solvent. As a result, one can conclude that the alkoxy substitutents are responsible for this behavior in fluorinated oligophenylenevinylenes.

Equation 1 describes the shift of fluorescence due to the formation of species that have a different charge distribution in the excited state in comparison to their electronic configuration in the ground state.[33,39] The behavior is similar to intramolecular

$$\nu_{CT} = \text{const.} - \frac{1}{4\pi hc\epsilon_0} \frac{2}{\rho^3} \mu_{CT}^{exc}(\mu_{CT}^{exc} - \mu_{CT}^{gs(FC)})\Delta f \quad (1)$$

charge-transfer states. For the sake of discussion, they will be called CT in this work. In eq 1, ν_{CT} is the emission energy in the corresponding solvent, ϵ_0 is the permittivity in a vacuum, Δf is the solvent polarity parameter,[33] ρ is the Onsager radius,[40] h is Planck's constant, μ_{CT}^{exc} is the dipole moment of the CT in the excited state, and μ_{CT}^{gs}(FC) is the dipole moment of the CT in the ground state with Franck–Condon geometry.

The slope obtained by using eq 1 is −13 300 cm^{-1}, indicating that the species formed in the excited state must have a different charge localization in comparison to that in the ground state. The slope is comparable with those published for a series of solvatochromic compounds, such as dialkylaminonaphthalene-

(28) Wadsworth, W. S.; Emmons, W. D. *J. Am. Chem. Soc.* **1961**, *83*, 1733.

(29) Horner, L.; Hoffmann, H. H.; Wippel, H. G.; Klahre, G. *Chem. Ber.* **1959**, *92*, 2499.

(30) Christian, G. D. *Analytical Chemistry*, 3 ed.; John Wiley & Sons: New York, 1980.

(31) Blatchford, J. W.; Gustafson, T. L.; Epstein, A. J.; Vanden Bout, D. A.; Higgins, D. A.; Barbara, P. F.; Fu, D.-K.; Swager, T. M.; MacDiarmid, A. G. *Phys. Rev. B* **1996**, *54*, R3683.
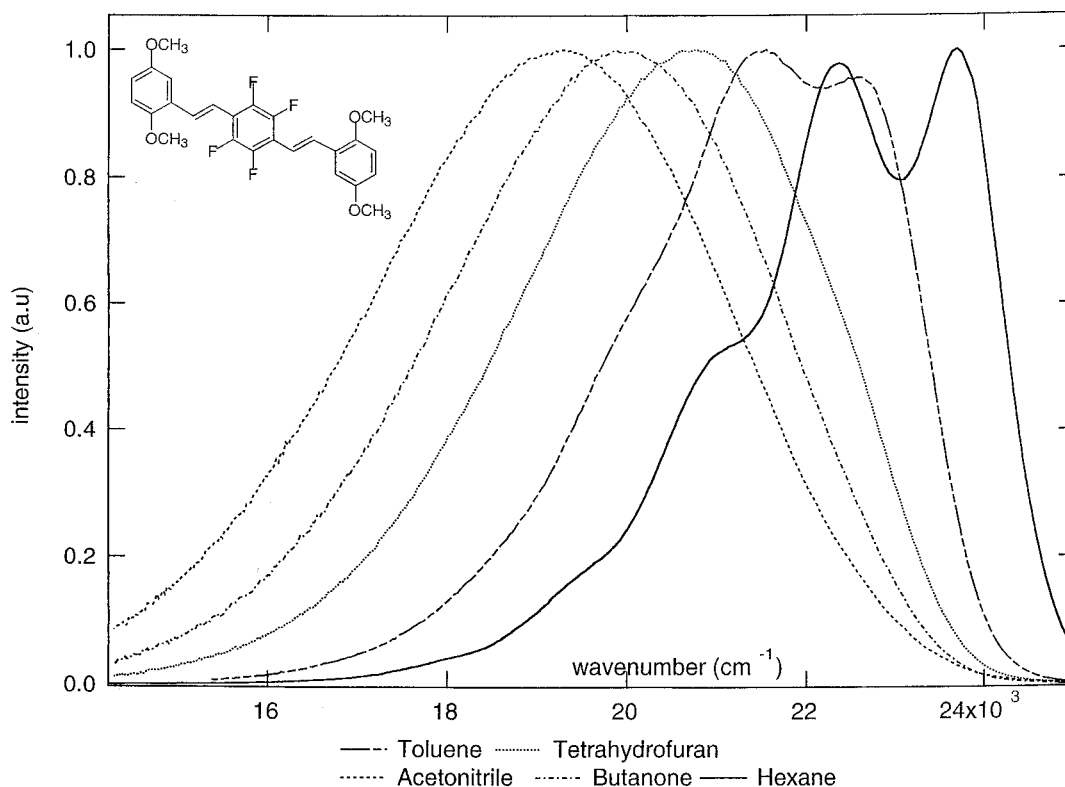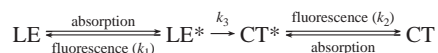
(32) Kavarnos, G. J. *Fundamentals of Photoinduced Electron Transfer*; VCH Publishers: New York, 1993.

(33) Baumann, W.; Bischof, H.; Fröhling, J.-C.; Brittinger, C.; Rettig, W.; Rotkiewicz, K. *J. Photochem. Photobiol. A: Chem.* **1992**, *64*, 49.

(34) Schuddeboom, W.; Jonker, S. A.; Warmann, J. M.; Leinhos, U.; Kühnle, W.; Zachariasse, K. A. *J. Phys. Chem.* **1992**, *96*, 10809.

(35) Zachariasse, K. A.; von der Haar, T.; Leinhos, U.; Kühnle, W. *J. Inf. Rec. Mater.* **1994**, *21*, 501.

(36) Leinhos, U.; Kühnle, W.; Zachariasse, K. A. *J. Phys. Chem.* **1991**, *95*, 2013.

(37) Jager, W. F.; Volkers, A. A.; Neckers, D. C. *Macromolecules* **1995**, *28*, 8153.

(38) Hoffmann, D. A.; Anderson, J. E.; Frank, C. W. *J. Mater. Chem.* **1995**, *5*, 13.

(39) Suppan, P.; Ghoneim, N. *Solvatochromism*; Royal Society of Chemistry: Cambridge, England, 1997.

(40) Onsager, L. *J. Am. Chem. Soc.* **1936**, *58*, 1486.

Figure 1. Fluorescence spectra of **6b** in solvents of different polarity

sulfonamides ($-10\,600$ cm^{-1} [37]) or coumarins ($-11\,300$ cm^{-1} [37]). These slopes are smaller in comparison to compounds forming an intramolecular charge transfer, such as dimethylamino-benzonitriles ($-24\,200$ cm^{-1} [33]) or dimethylaminobenzoic esters ($-27\,000$ cm^{-1} [33]). A quantitative evaluation requires knowledge of the Onsager radius, ρ, but this is unknown for **6b**. Onsager solvatochromic theory[40] also requires spheroid geometry, but this molecule's shape is more elliptic.

The spectra obtained for **6b** and **6d** in different solvents indicate the fluorescence of two emissive states that can be, in general, described by a reaction scheme that involves two species.[41] The large Stokes shift indicates that one of the states possesses a higher polarity (referred to as the charge-transfer state, CT* [42]), while the other undergoes no significant electron delocalization upon excitation and is referred to as the locally excited state, LE*. All other compounds having an alkyl substituent (**3c**, **3d**, **6c**) or only hydrogen on the aromatic ring (**3a**, **6a**) show no significant change in spectral shape as a function of solvent polarity. However, the decrease in the quantum yield is remarkable and indicates the formation of another state with small oscillator strength.

Charge transfer in **6b** and **6d** is possible due to substitution with electron-donating and -withdrawing substituents. Several charge-transfer models exist in the literature, though all require a geometry change in the excited state. One well-known model

is the formation of twisted intramolecular charge-transfer states (TICT).[43−47] TICT can occur by a perpendicular twist of two rotating molecule parts that is accompanied by charge transfer. The TICT mechanism has been examined using a series of dialkylaminobenzonitriles.[43−48] Other models involving formation of charge-transfer states discuss planarization of pretwisted molecule parts as it was shown for several 9,10-substituted biaryls[49,50] or the planarization of the dialkylamino group in the excited state[34−36] as an opposing mechanism to the TICT model. Planarization was also discussed for several cyano-substituted oligophenylenevinylene compounds.[6] These compounds had a pretwist of the phenyl rings due to the substitution at the olefinic group.

However, our quantum mechanical investigations show a planar molecule with C_{2h} symmetry. The results obtained make it obvious that planarization in the excited state could be one important reaction pathway. In addition, the formation of TICT states cannot be considered as the main path for charge transfer. For this reason, we could include additional models as the formation of polarons, which is important in understanding the photoluminescence in conjugated polymers.[51−53] In general, these species could be considered as dispersed polarons, as

(41) The photochemistry occurring in these compounds can be described in general with the following scheme including two species, the CT and the LE with their corresponding geometry in the ground and excited states (marked by the asterisk):

$$\text{LE} \underset{\text{fluorescence }(k_1)}{\overset{\text{absorption}}{\rightleftarrows}} \text{LE*} \xrightarrow{k_3} \text{CT*} \underset{\text{absorption}}{\overset{\text{fluorescence }(k_2)}{\rightleftarrows}} \text{CT}$$

The formation of CT* by LE* is assigned by the rate constant k_3. The validity of this mechanism has been approved by global analysis in the time-correlated single-photon counting.

(42) The asterisk is used when we report about the excited state. It is avoided in cases when the absorption of the ground state is considered.

(43) Rettig, W. *Angew. Chem.* **1986**, *98*, 969.

(44) Grabowski, Z. R.; Rotkiewicz, K.; Rubaszewska, W.; Kirkor-Kaminska, E. *Acta Phys. Pol.* **1978**, *A54*, 767.

(45) Grabowski, Z. R.; Rotkiewicz, K.; Siemiarczuk, A.; Cowley, D. J.; Baumann, W. *Nouv. J. Chim.* **1979**, *3*, 443.

(46) Grabowski, Z. R.; Rotkiewicz, K.; Siemiarczuk, A. *J. Lumin.* **1979**, *18/19*, 420.

(47) Rettig, W. In *Charge Transfer in Self-Decoupling π-Systems*; Rettig, W., Ed.; VCH−Publishers: New York, 1988; p 229.

(48) Lipinski, J.; Chojnacki, H.; Grabowski, Z. R.; Rotkiewicz, K. *Chem. Phys. Lett.* **1980**, *70*, 449.

(49) Schneider, F.; Lippert, E. *Ber. Bunsen-Ges. Phys. Chem.* **1968**, *74*, 624.

(50) Schneider, F.; Lippert, E. *Ber. Bunsen-Ges. Phys. Chem.* **1968**, *72*, 1155.

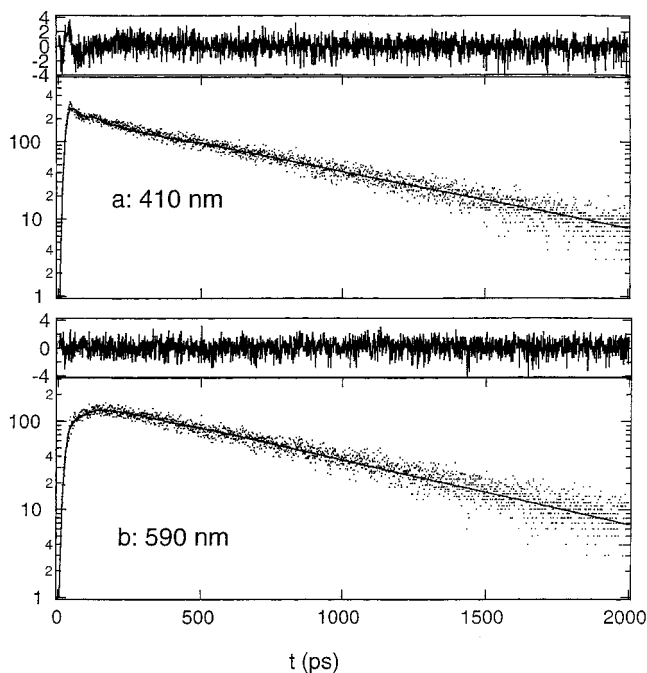(51) Soos, Z. G.; Ramasesha, S.; Galvao, D. S.; Etemad, S. *Phys. Rev. B* **1993**, *47*, 1742.

Figure 2. Plot for the fits obtained by global analysis for the emission of **6d** in toluene representing the decay in the blue part (upper) and red part (bottom). Eleven decays measured at 410, 420, 430, 450, 470, 490, 510, 530, 550, 570, and 590 nm were linked to one data set for global analysis; the χ^2 obtained for the global fit for all 11 linked decays was 1.109.

previously discussed for the tunneling effects in biological electron-transfer reactions.[54]

A recent theoretical study showed that the lowest excited state of complexes between two stilbene molecules had mostly intrachain character in its relaxed geometry.[55] It was concluded that the intrachain polaron−excitons are intrinsically the most stable photogenerated species. Furthermore, an additional amount of energy is necessary for dissociation of a polaron−exciton into a polaron pair, which is an extrinsic phenomenon.[55]

Emission Dynamics. The complexity of the solvent-dependent fluorescence spectra of **6b** and **6d** was analyzed in detail by global analysis[26] using a standard single-photon counting technique.[27] This treatment has recently become more popular for the analysis of complex photochemical reaction systems.[22−25]

A typical example is drawn in Figure 2 for the decay curves obtained, indicating that they can be globally described with two decay times over the entire spectrum. The upper decay represents the fluorescence behavior in the blue part of the spectrum, while the decay at the bottom is representative for the emission in the red part. The exponential decay behavior agrees well with the experimental data published during investigations of another polyphenylenevinylene oligomer in dimethyl sulfoxide.[56] A multiexponential decay behavior is more typical for solid-state photoluminescence.[10,31,52,57] Moreover, the fast decay obtained in the blue region is equal to the rise time in the red region. This agrees with the mechanism discussed in

(52) Kersting, R.; Mollay, B.; Rusch, M.; Wenisch, J.; Leising, G.; Kaufmann, H. F. *J. Chem. Phys.* **1997**, *106*, 2850.
(53) Dyakonov, V.; Frankevich, E. *Chem. Phys.* **1998**, *227*, 203.
(54) Warshel, A.; Chu, Z. T.; Parson, W. W. *Science* **1989**, *246*, 112.
(55) Cornil, J.; dos Santos, D. A.; Crispin, S.; Silbey, R.; Brédas, J. L. *J. Am. Chem. Soc.* **1998**, *120*, 1289.
(56) Katz, H. E.; Bent, S. F.; Wilson, W. L.; Schilling, M. L.; Ungashe, S. B. *J. Am. Chem. Soc.* **1994**, *116*, 6631.
(57) Vanden Bout, D.; Yip, W.-T.; Hu, D.; Fu, D.-K.; Swager, T. M.; Barbara, P. F. *Science* **1997**, *277*, 1074.

the previous section,[41] which requires a rise time for the CT* because it is formed from the LE* in the excited state.

Given that $k_1 + k_3 > k_2$, the time-dependent populations of the LE* and CT* excited states are described by eqs 2 and 3, respectively. Variables θ_1 and θ_2 are the eigenvalues of the

$$[LE]^*_t = a_{LE}(\lambda)[LE]^*_0 \exp(-\theta_1 t) \qquad (2)$$

$$[CT]^*_0 = b_{CT}(\lambda)\left(-\frac{[LE]^*_0 k_3}{\theta_1 - \theta_2}\exp(-\theta_1 t) + \left([CT]^*_0 + \frac{[LE]^*_0 k_3}{\theta_1 - \theta_2}\right)\exp(-\theta_1 t)\right) \quad (3)$$

differential equation system and, for the proposed mechanism, equal to the reciprocal decay times measured. This statement is true when the rate constant of the back reaction from the CT* to the LE* state is negligible. The terms $[LE]^*_0$ and $[CT]^*_0$ are equal to the zero time concentrations of the respective excited states. Rate constant k_3 describes the formation of the CT* in the excited state from the LE*. Variables $a_{LE}(\lambda)$ and $b_{CT}(\lambda)$ are, by definition, unknown functions for the spectra of each emitting state LE* and CT*. Despite the fact that θ_1 and θ_2 are directly related to the experimental decay times, eqs 2 and 3 have to be transformed into expressions containing the decay associated spectra (DAS)[25,58−60] in order to calculate $a_{LE}(\lambda)$ and $b_{CT}(\lambda)$ from the DAS data. The DAS are the measured preexponential coefficients except for a normalization factor and represent the contribution of each decay time at the corresponding wavelength.[61]

A plot of the ratio DAS_1/DAS_2 (Figure 3) gives information about the validity of a proposed mechanism.[25] The DAS concept was previously applied to check the validity of proposed photochemical reaction schemes.[25,58,59] The course for the ratio DAS_1/DAS_2 in Figure 3 indicates the validity of the proposed mechanism. The plot tends to go to infinity in the blue region of the spectrum. This behavior is caused by the fact that the contribution of the CT* to the emission is negligible in the blue region. Therefore, the wavelength-dependent factor $b_{CT}(\lambda)$ becomes zero, as does DAS_2.[25,58,59] This behavior of the DAS_1/DAS_2 ratio in the short-wavelength region is met only if no back-reaction occurs from CT* to LE* or, alternatively, if a back-reaction with a negligibly small rate occurs. Were there a

(58) Löfroth, J.-E. *Anal. Instrum.* **1985**, *14*, 403.
(59) Löfroth, J.-E. *J. Phys. Chem.* **1986**, *90*, 1160.
(60) The decay-associated spectra contain the preexponential factors α of the exponential functions that were used for the global fit analysis. They are wavelength dependent and are calculated using the following expression:

$$DAS(\lambda,\theta_i) = \frac{\alpha_i(\lambda)}{\sum\limits_{j=1}^{n}\dfrac{\alpha_i(\lambda)}{\theta_j}}ISS(\lambda)$$

where n is equal to the number of exponential functions used for the global fit and ISS(λ) corresponds to the intensity of the steady-state emission, and $\alpha_j(\lambda)$ are the preexponential factors obtained by the global fit.
(61) The analytical expression for the DAS can be obtained by adding up each coefficient of the exponential terms in the solution of the set of differential equation describing the photophysical model vertically, yielding

$$DAS_1 = a_{LE}(\lambda)[LE]^*_0 - \frac{b_{CT}(\lambda)[LE]^*_0 k_3}{\theta_1 - \theta_2} \quad \text{and}$$

$$DAS_2 = b_{CT}(\lambda)\left[[CT]^*_0 + \frac{[LE]^*_0 k_3}{\theta_1 - \theta_2}\right]$$
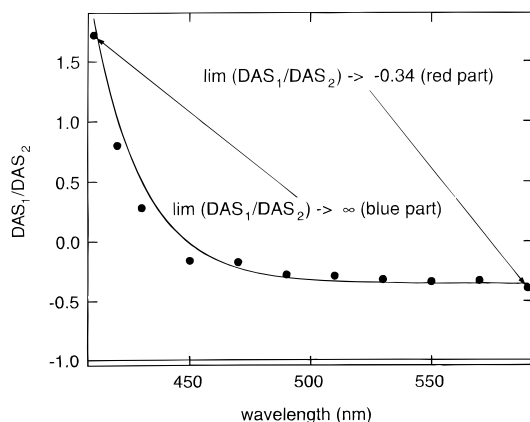
Figure 3. Plot of the ratio DAS_1/DAS_2 as a function of the wavelength for **6d** in toluene.

considerable contribution of a back-reaction in the excited state, the ratio DAS_1/DAS_2 would approach a constant value in the blue region of the spectrum. From other compounds[62] and simulations of photophysical reactions, we know that, in this case, the ratio DAS_1/DAS_2 exhibits a constant value in a very extended range on the blue side of the spectrum. The course of the ratio DAS_1/DAS_2 seen in Figure 3 does not show a constant value in the blue part of the spectrum. For this reason, we believe that the assumption of the tendency of the DAS ratio to approach infinity and the assumption of a negligible back reaction are justified. A view of the curve in the red region indicates a limiting value of -0.34. This number being larger than -1 and smaller than 0 shows that a reaction from LE* to CT* has to proceed; second, both states, the LE* and especially the CT*, need to have a considerable absorption from the ground state. If only the LE* were excited, the ratio of DAS_1/DAS_2 would have to approach the value of -1.

Furthermore, the DAS values obtained can be used to construct the spectra of the emitting species LE* and CT*. These are called species-associated spectra (SAS) and can be obtained by integration of eqs 2 and 3 over time, yielding eqs 4 and 5 as analytical expressions for $SAS_{LE}(\lambda)$ and $SAS_{CT}(\lambda)$, respectively.[63]

$$SAS_{LE}(\lambda) = \frac{DAS_1}{\theta_1} + \left[\cfrac{1}{1 + \cfrac{[CT]_0^*(\theta_1 - \theta_2)}{[LE]_0^* k_3}} \right] \frac{DAS_2}{\theta_1} \quad (4)$$

$$SAS_{CT}(\lambda) =$$
$$\left[\cfrac{1}{1 + \cfrac{[CT]_0^*(\theta_1 - \theta_2)}{[LE]_0^* k_3}} \left[1 + \frac{[CT]_0^* \theta_1}{[LE]_0^* k_3} \right] \right] \frac{\theta_1 - \theta_2}{\theta_1 \theta_2} DAS_2 \quad (5)$$

SAS are drawn for the LE* and CT* in Figure 4. The data confirm the results obtained from the steady-state spectra. The fluorescence of these compounds is a sum of two emissions that can be attributed to one polar and one nonpolar species, and the shoulder in the steady-state spectrum is also explained. Moreover, the shape of the spectrum obtained for LE* shows the fine structure of the emission that is representative for many aromatic compounds.[64] This spectral shape was also obtained

(62) Seifert, H.; Rettig, W. *Global Analysis of Fluorescence Decay Traces for Excited-State Reactions*; Conf. Proc., 4th Conference on Methods and Applications of Fluorescence Spectroscopy, Robinson College, Cambridge, UK, September 24−27, 1995.
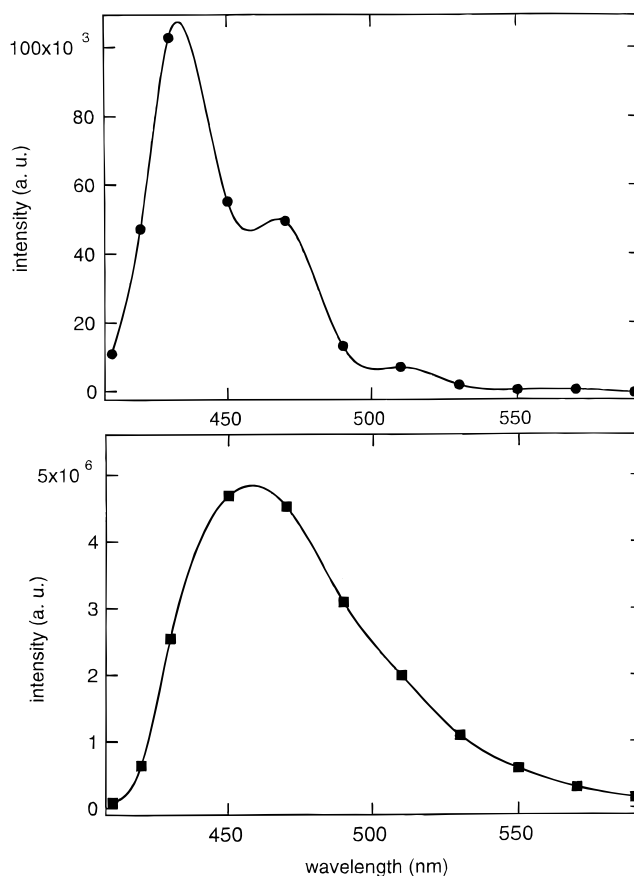

Figure 4. SAS spectra for the LE and CT state and the steady spectrum of **6d** in toluene.

using less polar solvents than toluene (e.g., cyclohexane, $E_T^N(\text{cyclohexane}) = 0.006$,[65] $E_T^N(\text{toluene}) = 0.099$[65]) and for all other compounds containing no alkoxy substitution (**3a**, **3c**, **3d**, **6a**, and **6c**). In other words, the alkoxy substitution of fluorinated oligophenylenevinylenes is connected with the formation of the CT*-state, and this has a remarkably high contribution to the overall fluorescence. Other CT systems, such as the intramolecular charge transfer in dimethylaminobenzonitriles, indicated a considerably lower amount of CT* emission in the fluorescence spectra[33−36,43−48] in nonpolar solvents.

The results obtained by global analysis in toluene can be confirmed by measurements in solvents having a different polarity. These are compiled in Table 2 for various solvents of different solvent polarity.

The slowest formation of the CT was observed in *n*-hexane, which has the lowest polarity. This result shows correlation

(63) For the calculation of the SAS from the DAS obtained from the experiment the limiting value of the ration DAS_1/DAS_2 in the long wavelength region is used. It is given by

$$\lim_{\lambda \to \infty} \frac{DAS_1}{DAS_2} - \cfrac{1}{1 + \cfrac{[CT]_0^*(\theta_1 - \theta_2)}{[LE]_0^* k_3}}$$

Furthermore, the ratio $[CT]_0^*/[LE]_0^* k_3$ can be calculated from this limit. Both parameters can be substituted into eqs 4 and 5 to obtain the SAS data for the emitting species CT* and LE*.

(64) Birks, J. B. *Organic Molecular Photophysics*; John Wiley & Sons: New York, 1975.

(65) Reichardt, C. *Solvents and Solvent Effects in Organic Chemistry*; VCH: New York, 1988.

(66) Lide, D. R.; Frederikse, H. R. R. *CRC Handbook of Chemistry and Physics, A Ready Reference of Chemical and Physical Data*; CRC Press: Boca Raton, FL, 1997; Vol. 78.

Table 2. Summary of the Fluorescence Data and Comparison with Solvent Data Such as Polarity and Viscosity for **6d** Obtained for Global Analysis in *n*-Hexane, Toluene, and Acetonitrile

| solvent	τ_1 (ps)	τ_2 (ps)	lim DAS$_1$/DAS$_2$ (red)	ϵ	η (mPa·s)
n-hexane	381	1281	−0.20	1.88[a]	0.28[b]
toluene	101	1590	−0.34	2.38[a]	0.52[b]
acetonitrile	27	2974	−0.90	35.94[a]	0.33[b]

[a] Reference 65.   [b] Reference 66.

between the kinetics of CT* formation and the solvent used. On the other hand, viscosity does not significantly influence the kinetics. All three solvents selected have approximately the same viscosity. Therefore, translational processes (for example, formation of dimers or intermolecular charge transfer) should be insignificant for the reaction pathways of the excited state in dilute solution because these processes rely more on the viscosity of the surrounding solvent.

The data for the ratio DAS$_1$/DAS$_2$ obtained by extrapolation in the red region of the emission spectrum signifies a considerably large contribution of CT. The transition from the ground state to a state with charge-transfer character should be forbidden. The energy difference between both states seems to be so small in **6d** that the charge-transfer state can gain oscillator strength from the LE state. This model would account for the considerable contribution of the CT state to the absorption spectrum observed by the global analysis and for the blue shift of the absorption spectrum with increasing solvent polarity. Table 2 shows that the contribution of the CT absorption decreases with increasing solvent polarity, because the long wavelength limit of the ratio DAS$_1$/DAS$_2$ decreases from −0.2 in *n*-hexane to −0.9 in acetonitrile. A value of this limit close to −1 indicates that only one species, the LE state for our model, absorbs. This diminished contribution of the CT absorption on the red side of the total absorption spectrum is one reason for the blue shift of that spectrum. In the more polar solvents, the CT* state is stabilized, and the energetic difference between the two states increases. This leads to a loss in oscillator strength of the LE* which is gained by the CT* and results in the bathochromic shift seen for the emission. Furthermore, the LE ground state can be stabilized more as the solvent polarity increases.[39] This could also account for the hypsochromic shift observed.

The lifetime of the CT* indicates the expected dependence on solvent polarity. This phenomenon is due to the different solvation effects and can be used to probe several materials. The kinetic data do not agree with the dipole relaxation of the matrix. These numbers are some orders of magnitude faster than the data reported about the kinetics for CT* formation in this work (average τ values measured for the solvation dynamics: acetonitrile ≈ 0.22 ps[67] and toluene ≈ 1.3 ps[68]). For this reason, it can be assumed that the solvent molecules are in an equilibrium distribution around the solute during the whole reaction. Therefore, the reaction is not driven by the reorientation of the solvent molecules around the excited-state dipoles. The charge-transfer state has its own deactivation characteristics when it is formed. It has to be a molecule with a polarized charge distribution due to the strong Stokes shift observed in the steady-state spectra.

Influence of Substitution on Solid-State Behavior. Polarization microscopy indicates birefringence in the molten state during heating and cooling cycles for **3b** and **6d**. The crossed
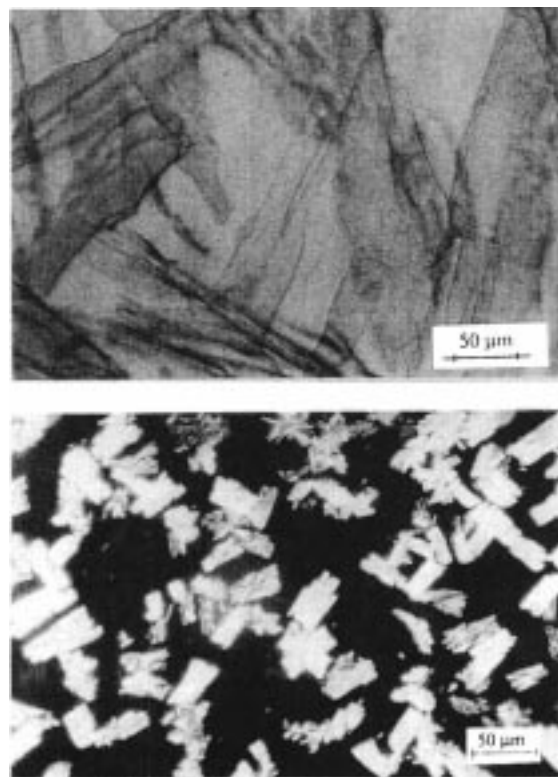
Figure 5. Optical micrographs for **3b** in the molten state obtained under crossed polarizers during heating at 88 °C (top) and cooling at 60 °C (bottom) in the first cycle.

polarized micrographs obtained are shown for **3b** in Figure 5 and for **6d** in Figure 6. The textures obtained are different for both compounds. All other compounds investigated in this work show no birefringence in the molten state.

Compound **3b** shows birefringence during the heating cycle and rodlike particles during the cooling cycle, which are different from its crystalline feather structures. The texture in Figure 5a is comparable with that of copper phthalocyanines having benzyloxyethoxy side chains,[69] which are reported to form a discotic phase.

Compound **6d** shows birefringent behavior during the heating cycle with the texture shown in Figure 6a. During cooling, this compound shows components of a texture in Figure 6b and c that are comparable with structures found in smectic[70] and in discotic[71−74] mesophases. A similar texture was also found in branched liquid crystalline polyethers containing cyclotetraveratrylene-based disklike mesogens.[71] The growth of the domains can be seen during additional cooling, switching from Figure 6b to Figure 6c if one examines the size of the domains. Figure 6c, shows two coexistent phases containing still the components shown in Figure 6b.

Stacking[75] has also recently been reported for **6a**,[16] but this compound shows no birefringence in the molten state. Stacking

(67) Maroncelli, M. *J. Chem. Phys.* **1997**, *106*, 1545.
(68) Reynolds, L.; Gardecki, J. A.; Frankland, S. J. V.; Horng, M. L.; Maroncelli, M. *J. Phys. Chem.* **1996**, *100*, 10337.

(69) Osborn, E. J.; Schmidt, A.; Chau, L.-K.; Chen, S.-Y.; Smolenyak, P.; Armstrong, N. R.; O'Brien, D. F. *Adv. Mater.* **1996**, *8*, 926.
(70) Demus, D.; Richter, L. *Textures of liquid crystals*; Deutscher Verlag für Grundstoffindustrie: Leipzig, 1980.
(71) Percec, V.; Cho, C. G.; Pugh, C.; Tomazos, D. *Macromolecules* **1992**, *25*, 1164.
(72) Corsellis, E. A.; Coles, H. J.; Mckeown, N. B.; Weber, P.; Guillon, D.; Skoulios, A. *Liq. Cryst.* **1997**, *23*, 475.
(73) Destrade, C.; Foucher, P.; Gasparoux, H.; Tinh, N.; Levelut, A. M.; Malthete, J. *Mol. Cryst. Liq. Cryst.* **1984**, *106*, 121.
(74) Destrade, C.; Huu Tinh, N.; Gasparoux, H.; Malthete, J.; Levelut, A. M. *Mol. Cryst. Liq. Cryst.* **1981**, *71*, 111.
(75) Alkorta, I.; Rozas, I.; Elguero, J. *J. Org. Chem.* **1997**, *62*, 4687.

Table 3. Results of DSC Measurements of **3a−d** and **6a−d** Indicating the Peak Maximum, T_{max}, Enthalpy, ΔH, and Entropy, ΔS, for the Phase Transition

	heating						cooling					
	T_{max} (°C)		ΔH (kJ mol⁻¹)		ΔS (J mol⁻¹ K⁻¹)		T_{max} (°C)		$-\Delta H$ (kJ mol⁻¹)		$-\Delta S$ (J mol⁻¹ K⁻¹)	
	run 1	run 2	run 1	run 2	run 1	run 2	run 1	run 2	run 1	run 2	run 1	run 2
3a	197.6	196.5	3.9	4.5	8	10						
	214.6	214.4	42.2	42.6	87	87	204.9	205.3	42	42	88	87
3b	80.5		49.3		139		63.7	61.4	1.9	1.9	6	6
	87.2	85.8	8.9	22.1	25	61	58.0	55.5	21.7	22.7	66	69
3c	168.9	211.9	4.1		9							
	211.8		43.3	42.8	89	88	201.2	200.7	41.4	41.8	87	88
3d	108.3	107.2	51.1	48.3	134	127	68.0	67.7	50.5	50.7	148	149
6b	143.6		5.0		12							
	220.9	220.7	42.7	42.1	86	85	178.3	182.3	37.0	37.7	82	83
6c	156.0		2.1		5							
	188.9	188.9	39.2	42.1	85	91	157.4	155.2	42	41	97	96
6d	60.3	80.5	40.2	1.3	121	4	108.6	107.6	21.6	21.9	57	58
	104	105	8.6	8.5	23	23	93.7	93.6	10.8	11.2	30	30
	126.4	126.2	19.5	19.0	49	48	77.4	77.4	0.9	1.4	3	4
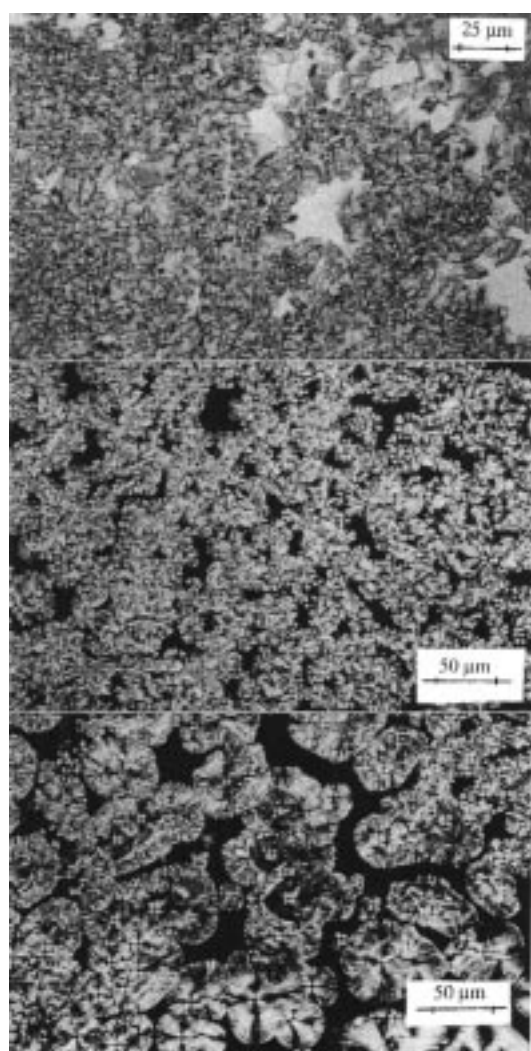
Figure 6. Optical micrographs for **6d** in the molten state obtained under crossed polarizers during heating at 114 °C (top) and cooling at 105 (middle) and 94 °C (bottom) in the first cycle.

of these molecules in combination with longer alkoxy chains substituted at the middle phenylene ring (**3b**) or the outer phenylene rings (**6d**) of the oligophenylenevinylenes can be discussed as one reason for the formation of the mesomorphic behavior, observed. Compound **3d** shows no mesomorphic behavior, although this compound possesses a long alkyl chain

at the middle phenylene ring. Possibly the alkyl chains of **3d** have a smaller effect on mesophase formation in comparison to the alkoxy chain of **3b**. Alkyl substituents do not have sufficient flexibility for mesomorphic behavior. On the other hand, alkoxy groups with a long chain allow formation of mesophases.

The results from the polarization microscopy experiments were supported by DSC measurements (see Table 3). Compounds **3b** and **6d** show several phase transitions in both the first heating and cooling scans, as well as the second scan. It should be noted that the entropy change for **3b** is considerably higher for the transition from the liquid crystalline into the crystalline state when compared to the transition from the isotropic state into the liquid crystalline one. In contrast to this, the entropy change in the case of **6d** is lower from the crystalline to the liquid crystalline state in comparison to the transition from the liquid crystalline to the isotropic state. A comparison of the enthalpies and entropies for **3b** and **6d** shows that they lie in the same range as reported for the phase transitions from crystalline to discotic[71,76−78] or smectic,[79] and from the discotic state to the isotropic state.[71,76−78] The other compounds do not show multiple transitions during heating and cooling. Some of these compounds show more than one peak only during heating. Since perfluoro compounds are able to form π-stacked aggregates,[16,18,75] these aggregates may be influenced by temperature, causing these extraneous peaks. Therefore, further enthalpy changes measured by DSC may be a result of changes in the aggregates formed.

The formation of ordered structures can be considered as one reason for observation of the extremely red shifted fluorescence cast film of the oligomer itself. Figure 7 shows the emission spectra of **3b** and **6d** in a cast film. The strong bathochromic shift of **3b** (>120 nm) in the film can be explained by the presence of aggregates that can have an ordered structure. A similar behavior was found in the case of **6d**, although the spectrum of this compound shows some blue-shifted structures. The differences in these spectra can be explained by the formation of different ordered structures in the solid state. Therefore, we can conclude that the molecular architecture of the oligomer itself should have a tremendous influence on the emission behavior in cast film.

(76) Milgrom, L. R.; Yahioglu, G.; Bruce, D. W.; Morrone, S.; Henari, F. Z.; Blau, W. J. *Adv. Mater.* **1997**, *9*, 313.

(77) Raja, K. S.; Ramakrishnan, S.; Raghunathan, V. A. *Chem. Mater.* **1997**, *9*, 1630.

(78) Collard, D. M.; Lillya, C. P. *J. Am. Chem. Soc.* **1991**, *113*, 8577.

(79) Strehmel, V. *J. Polym. Sci., Polym. Chem.* **1997**, *35*, 2653.
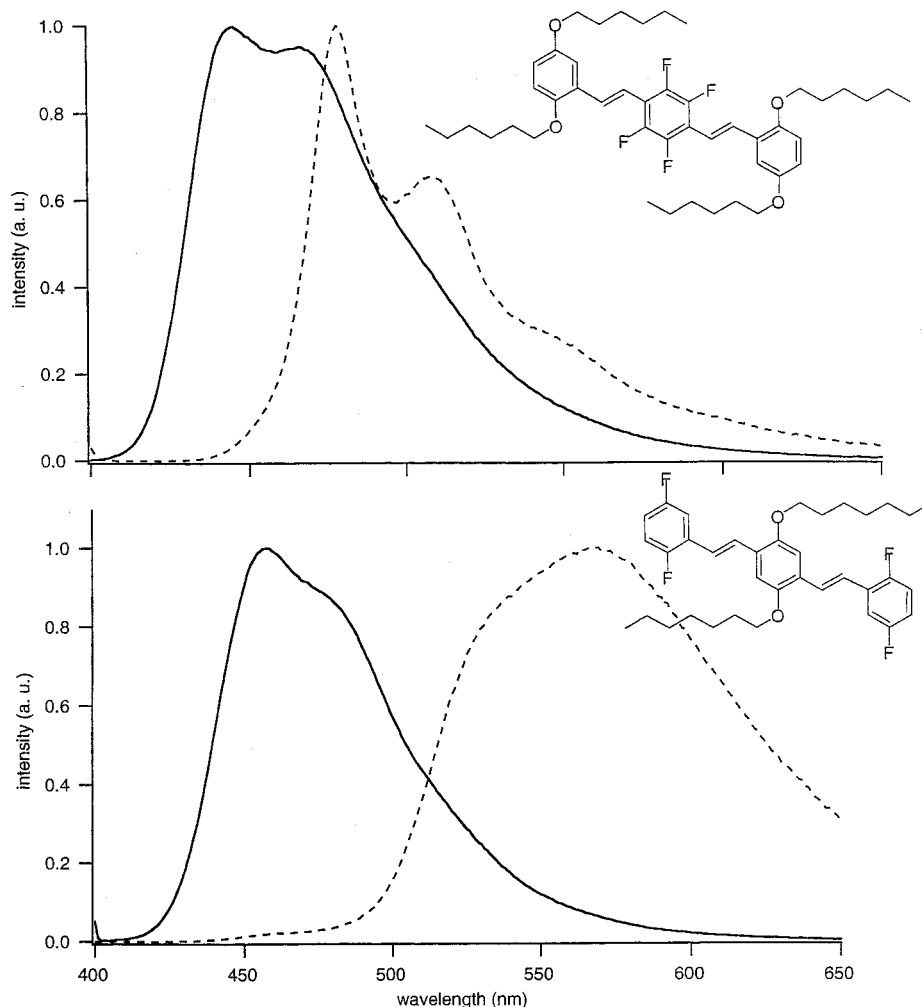
Figure 7. Fluorescence spectra of the compounds **3b** and **6d** in cast films.

Conclusions

Fluorinated oligo(*p*-phenylenevinylene)s with alkoxy substituents show new directions for the development of devices and fluorescent probes. The dominating emission of the charge-transfer state is strongly solvent dependent and can be used to probe molecular environments for several organic materials and synthetic polymers in order to get information about polarity. Furthermore, the ordered structure formed for long alkoxy chain derivatives might be responsible for the strong red-shifted photoluminescence of the neat material in films, which is of great interest for light-emitting diodes. Modifying the terminus of the alkoxy chain with hydrophilic groups could yield interesting compounds, which could be used to manufacture Langmuir−Blodgett films and make multilayered devices. Previously it was shown that discotic structures can be obtained with the Langmuir−Blodgett−Kuhn technique.[80] Furthermore, functionalizing the terminus of the alkoxy chain with surface-reactive groups such as thiol, trichlorosilyl, or trialkoxysilyl gives the opportunity to make self-assembled monolayers.[81]

Photoreactions, such as the [2 + 2] cycloaddition of the double bond, should yield an ordered phase that is insoluble and cross-linked. Cross-linking of liquid crystalline monomers in order to obtain ordered polymer networks has gained importance, as it was recently shown for the cross-linking of acrylic esters[82] or epoxides.[79] Our compounds open new directions for this technology. The discotic alignment for some of these compounds should yield sufficient efficiencies for the ordered cross-linked photoproducts without the addition of any initiator because the fluorinated oligophenylenevinylene is reactive enough to form such materials.

Experimental Section

Synthesis of the Materials. General Information. All manipulations were performed under an inert argon atmosphere using standard techniques. Reagents and solvents were purchased from Aldrich and used without further purification.

NMR spectra were taken with a Varian Gemini 200 NMR spectrometer. GC/MS were taken on a Hewlett-Packard 5988 mass spectrometer coupled to an HP 5880A GC with a 30-m × 0.25-mm-i.d. × 0.25-mm film thickness DB-5 MS column (J & B Scientific), interfaced to an HP 2623A data processor. UV−visible spectra were obtained using an HP 8452 diode array spectrophotometer. Molar absorption coefficients were taken from the maximum in toluene. Infrared spectrometry was performed using a Mattson Instruments 6020 Galaxy series FT-IR spectrometer. High-resolution mass spectra were obtained from the Mass Spectrometry Laboratory in the University of Illinois at Urbana−Champaign. Thin-layer chromatography was performed on Sigma-Aldrich plates (layer thickness, 250 μm; particle size, 5−17 μm; pore size, 60 Å) purchased from Aldrich. Silica gel

(80) Jutile, A.; Janietz, D.; Reiche, J.; Lemmetyinnen, H. *Thin Solid Films* **1995**, *268*, 121.

(81) Sagiv, J. *J. Am. Chem. Soc.* **1980**, *102*, 92.

(82) Hikmet R. A. M.; Kemperman, H. *Nature* **1998**, *392* (6675), 476.

chromatography was performed using silica gel (40 μm, 32−63 μm) purchased from Scientific Adsorbents Inc. Melting points were determined using a capillary melting point apparatus (Uni-melt, Arthur H. Thomas Co., Philadelphia, PA).

General Procedure for Synthesis of *trans,trans*-1,4-Bis[2-(2′,5′-difluoro)phenylethenyl]benzene Compounds (3a−d). To a cooled solution (0 °C) of NaH (6 equiv, prewashed with hexanes) in THF (1 M) was added dropwise via cannula a solution of the corresponding dialdehyde (1 equiv) and phosphonate (2.1 equiv) in THF (0.33 M with respect to phosphonate). The solution was monitored by TLC until completion. The solution was carefully quenched with water and extracted with ether. In some cases, the product crystallized from the ether solution, and the crystals were filtered and collected. The ether layer was dried over MgSO$_4$ and concentrated. Purification was achieved via silica gel chromatography or recrystallization, depending on the solubility of the specific compound.

***trans,trans*-1,4-Bis[2-(2′,5′-difluoro)phenylethenyl]benzene (3a).** This compound was isolated in 67% yield as bright yellow crystals from the ether extraction layer: ^{1}H NMR (DMSO) δ 7.67 (s, 2H), 7.64−7.76 (m, 1H), 7.45 (d, *J* = 16.4 Hz, 1H), 7.28 (d, *J* = 16.6 Hz, 1H), 7.16−7.36 (m, 2H); IR (neat) 1489, 956, 795; MS (EI) 354, 214, 177; HRMS (M$^+$) calculated for C$_{22}$H$_{14}$F$_4$: 354.1032, found 354.1028; mp = 212−215 °C; lg ϵ = 4.66 M^{-1} cm^{-1}.

***trans,trans*-1,4-Bis[2-(2′,5′-difluoro)phenylethenyl]-2,5-diheptyloxybenzene (3b).** Silica gel chromatography (20:1 hexanes/ethyl acetate) provided bright yellow crystals in 96% yield: ^{1}H NMR (CDCl$_3$) δ 7.50 (d, *J* = 16.8 Hz, 1H), 7.28−7.36 (m, 1H), 7.28 (d, *J* = 17.2 Hz, 1H), 7.12 (s, 1H), 6.82−7.05 (m, 2H), 4.07 (t, *J* = 9.3 Hz, 2H), 0.86−1.92 (m, 13H); IR (neat) 2926, 1489, 970; MS (EI) 582, 386; TLC (hexanes/ethyl acetate 20:1) R_f = 0.25; MS (EI) 582, 386, 141; HRMS (M$^+$) calculated for C$_{36}$H$_{42}$O$_2$F$_4$, 582.3121, found 582.3108; mp = 85−88 °C; lg ϵ = 4.53 M^{-1} cm^{-1}.

***trans,trans*-1,4-Bis[2-(2′,5′-difluoro)phenylethenyl]-2,5-dimethylbenzene (3c).** Filtration of the reaction mixture provided bright yellow crystals in 75% yield. These crystals could be further purified by chromatography (hexanes/ethyl acetate 20:1): ^{1}H NMR (CDCl$_3$) δ 7.46 (s, 1H), 7.36 (d, *J* = 16.6 Hz, 1H), 7.24−7.35 (m, 1H), 7.13 (d, *J* = 16.6 Hz, 1H), 6.92−7.09 (m, 2H), 2.45 (s, 3H); IR (neat) 2924, 959, 798; TLC (hexanes/ethyl acetate 10:1) R_f = 0.48; MS (EI) 382, 127; HRMS (M$^+$) calculated for C$_{24}$H$_{18}$F$_4$, 382.1345, found 382.1339; mp = 205−208 °C; lg ϵ = 4.62 M^{-1} cm^{-1}.

***trans,trans*-1,4-Bis[2-(2′,5′-difluoro)phenylethenyl]-2,5-dioctylbenzene (3d).** After concentration of the organic layer, this compound was passed through a short column of silica gel (hexanes/ethyl acetate 20:1) and then recrystallized from ethanol to give bright yellow crystals in 63% yield: ^{1}H NMR (CDCl$_3$) δ 7.45 (s, 1H), 7.41 (d, *J* = 15.4 Hz, 1H), 7.24−7.33 (m, 1H), 7.13 (d, *J* = 15.4 Hz, 1H), 6.92−7.09 (m, 2H), 2.76 (t, *J* = 8.0 Hz, 2H), 1.26−1.63 (m, 12H), 0.84−0.87 (m, 3H); IR (neat) 2919, 1495, 1090, 956; TLC (hexanes/ethyl acetate 20:1) R_f = 0.44; MS (EI) 578, 367, 127; HRMS (M$^+$) calculated for C$_{38}$H$_{46}$F$_4$, 578.3536, found 578.3530; mp = 105−107 °C; lg ϵ = 4.59 M^{-1} cm^{-1}, λ_{max} = 356 nm.

General Procedure for Synthesis of *trans,trans*-1,4-Bis(2-phenylethenyl)-2,3,5,6-tetrafluorobenzene Compounds (6a−d). To a cooled solution (0 °C) of NaH (6 equiv, prewashed with hexanes) in THF (1 M) was added dropwise via cannula a solution of the diphosphonate (1 equiv) in THF (0.15 M). The mixture was allowed to stir for 30 min, and then a solution of the aldehyde (2.05 equiv) in THF (0.5 M) was added via cannula. The reaction was monitored by TLC until completion. The solution was carefully quenched with water and extracted with ether. In some cases, the product crystallized from the ether solution, and the crystals were filtered and collected. The organic layer was dried over MgSO$_4$ and concentrated. Purification was achieved via silica gel chromatography or recrystallization, depending on the solubility of the specific compound.

***trans,trans*-1,4-Bis(2-phenylethenyl)-2,3,5,6-tetrafluorobenzene (6a).** This compound was filtered from the organic layer and chromatographed over silica gel (hexanes/benzene 30:1) to provide pale yellow crystals in 60% yield: ^{1}H NMR (C$_6$D$_6$) δ 7.49 (d, *J* = 16.8 Hz, 1H), 7.21−7.26 (m, 2H), 7.05−7.11 (m, 3H), 7.02 (d, *J* = 16.8 Hz, 1H); IR

(neat) 2922, 1480, 1092, 967; TLC (hexanes/ethyl acetate 10:1) R_f = 0.55; MS (EI) 354, 314, 177; mp = 208−210 °C dec (lit.[16] mp = 216 °C); lg ϵ = 4.61 M^{-1} cm^{-1}.

***trans,trans*-1,4-Bis[2-(2′,5′-dimethoxy)phenylethenyl]-2,3,5,6-tetrafluorobenzene (6b).** This compound was filtered from the organic layer and recrystallized from benzene to provide orange-yellow crystals in 97% yield: ^{1}H NMR (CDCl$_3$) δ 7.82 (d, *J* = 16.8 Hz, 1H), 7.14 (s, 1H), 7.09 (d, *J* = 17.2 Hz, 1H), 6.87 (s, 1H), 6.86 (s, 1H), 3.86 (s, 3H) 3.83 (s, 3H); IR (neat) 2948, 1490, 1218, 975; MS (EI) 474, 431, 237; HRMS (M$^+$) calculated for C$_{26}$H$_{22}$O$_4$F$_4$, 474.1454, found 474.1453; mp = 219−220 °C; lg ϵ = 4.63 M^{-1} cm^{-1}.

***trans,trans*-1,4-Bis[2-(2′,5′-dimethyl)phenylethenyl]-2,3,5,6-tetrafluorobenzene (6c).** This compound was filtered from the organic layer and recrystallized from chloroform to provide bright yellow crystals in 61% yield: ^{1}H NMR (CDCl$_3$) δ 7.74 (d, *J* = 16.4 Hz, 1H), 7.45 (s, 1H), 7.08 (AB quartet, ν_A = 7.11, ν_B = 7.05, J_{AB} = 11.7 Hz, 2H), 6.97 (d, *J* = 16.8 Hz, 1H), 2.39 (s, 3H), 2.38 (s, 3H); IR (neat) 2919, 1097, 971; MS (EI) 410, 205, 115; HRMS (M$^+$) calculated for C$_{26}$H$_{22}$F$_4$, 410.1658, found 410.1666; mp = 184−186 °C; lg ϵ = 4.64 M^{-1} cm^{-1}.

***trans,trans*-1,4-Bis[2-(2′,5′-dihexyloxy)phenylethenyl]-2,3,5,6-tetrafluorobenzene (6d).** This compound was filtered after putting the reaction mixture into ice−water and recrystallized from chloroform to provide yellow crystals in 84% yield: ^{1}H NMR (CDCl$_3$) δ 7.82 (d, *J* = 17 Hz, 2H), 7.136 (s, 2H), 6.84 (s, 4H), 3.96 (m, 8H), 1.79 (m, 8H), 1.51−1.25 (m, 24H); MS (EI) 755, 418, 209; HRMS (M$^+$) calculated for C$_{46}$H$_{62}$O$_4$F$_4$, 754.4584, found 754.4568; mp = 103−105 °C; lg ϵ = 4.59 M^{-1} cm^{-1}.

Physical Methods and Calculations for the Examination of the Materials. (i) Fluorescence Measurements. (a) Stationary Fluorescence. Fluorescence spectra were recorded with a Spex Fluorolog 2 equipped with both excitation and emission double-beam monochromators. All spectra were corrected (band-pass, 2.8 nm). Solution spectra were measured in perpendicular geometry using 1-cm quartz cuvettes. Front face detection was applied to collect all spectra in thin films. All fluorescence quantum yields are relative to 9,10-diphenylanthracene in cyclohexane as external the standard[83] (Φ_f = 0.9). All solutions were air saturated. Fluorescence spectra of cast films were recorded by using front face geometry.

(b) Time-Correlated Single-Photon Counting. Fluorescence lifetimes were measured by using standard single-photon techniques.[27] A BeamLokTM 2080 argon ion laser was combined with a Ti−Safire Tsunami laser (both from Spectra Physics) to produce pulses with a half-width of about 50 fs and a frequency of 81.47 MHz at 387 nm. A monochromator MS 257 from L.O.T. Oriel (Darmstadt, Germany) was used to select the desired detection wavelength; the band-pass was between 2 and 16 nm, depending on the position of the registration. All decay curves were measured with a magic angle polarizer in order to eliminate polarization effects.

The single-photon counting electronics contained the following parts: a fast signal amplifier, constant fraction discriminator TC454 (Quad) from Tenelec, time amplitude converter TC864 from Tenelec (TAC/Biased Amplifier), a multichannel analyzer PC card from FAST ComTec (MCDLAP), and a trigger diode AR-S1S from Antel. A microchannel plate R1564-U01 from Hamamutsu was taken for the detection.

(ii) Thermoanalytical Characterization of the Materials. All DSC measurements were carried out with a Perkin-Elmer DSC-7. A heating and cooling rate of 10 K/min was chosen for all measurements. For polarization microscopic investigations, a polarization microscope Jenapol U was used for all measurements. It was equipped with a long distance objective 25/50. The samples were heated in a Linkam heating chamber. The heating and cooling rate was 10 K/min. All samples were heated until the isotropic state was reached.

Preparation of the Films. A 0.5-mL portion of a 10 wt % solution of the oligophenylenevinylene compound in toluene was coated on a glass slide (same size as above). The cast film dried in the solvent atmosphere for 24 h to obtain the desired material.

(83) Sanyo, H.; Hirayama, F. *J. Phys. Chem.* **1983**, *87*, 83.

Quantum Mechanical Calculations. MOPAC 93 from Fujitsu was taken for all semiempirical calculations using the PM3 Hamiltonian.

JA983308N